

Figure 1 VERMIX station map of the five transects in the northeastern North Sea overlain on (a) surface chlorophyll a (mg chl m^{-3}) and (b) sea surface temperature ($^{\circ}\text{C}$) from MODIS satellite images (4 km resolution) obtained 20 July 2016 (clouds are shown in dark gray). (a) CTD stations (bullets) and stations where ^{14}C -incubations for primary production were used for estimating photosynthetic parameters in the area (white circles) along the five transects (Tr1-5). Horizontal yellow bars (Tr2-5) show the separation between nitrate-deplete and nitrate-replete areas. Water masses in the area are indicated (see text). Bathymetry is contoured in meters.

Figure 2 Distributions along Tr4 of (a) potential temperature ($^{\circ}\text{C}$, colours and white contours, additional contours above 16 $^{\circ}\text{C}$ in 0.5 $^{\circ}\text{C}$ intervals), (b) salinity (psu, colours and white contours, additional contours between 26-34 in 0.5 psu intervals) and contours of potential density anomalies (intervals of 1 kg m^{-3} , orange lines), (c) oxygen ($\mu\text{mol kg}^{-1}$, colours and black contours) and (c) nitrate ($\mu\text{mol kg}^{-1}$, colours and white contours and orange contours of potential density anomalies as in b). Vertical lines show location of the CTD-measurements.

Figure 3 Distributions of chlorophyll a (mg chl m^{-3} , colours and black contours, additional white contours are shown in intervals of 2 mg chl m^{-3}) along Tr1-Tr5 (a-e). Nutricline depths (red bullets) and depths with maximum nitrate flux into the euphotic zone (orange squares) were calculated at each station where water samples (black triangles) and turbulence profiles were made, respectively. Contours of potential density anomalies are shown in intervals of 1 kg m^{-3} (orange lines). Note the different latitude-intervals in the figures.

Figure 4 (a) Potential temperature-salinity diagram of all CTD-measurements and (b) a high-saline subset of the measurements (small grey bullets). Water sample concentrations of nitrate are shown with large bullets in (a,b) ($\mu\text{mol kg}^{-1}$, colour bar). Contour lines show isopycnals of potential density anomalies and selected water masses are indicated. (c) Nitrate vs phosphate for all water samples. The total water depth is shown with colours (m) and the relationship $[\text{NO}_3^-] = \eta_{\text{N:P}} [\text{PO}_4^-]$, $\eta_{\text{N:P}} = 16:1$, is shown with a grey dashed line.

Figure 5 Turbulence measurements along Tr2 (a,c) and Tr4 (b,d). (a,b) Logarithm (Log_{10}) of dissipation of turbulent kinetic energy (W kg^{-1}) and (c,d) calculated vertical turbulent diffusion coefficient ($\text{m}^2 \text{s}^{-1}$).

Figure 6 Vertical profiles from four stations across the shelf edge of (upper panels) potential density anomaly, chlorophyll a and nitrate (bullets) and (lower panels) dissipation of TKE (average value and values from the two shear sensors are shown with bullets and open circles, respectively), Brunt-Väisälä frequency (dashed line), turbulent diffusion coefficient and the vertical turbulent nitrate flux. The nutricline depth (D_{NO_3}) and depth of the euphotic zone (0.1% PAR) are shown (dashed and dotted lines) and station information of locations, D_{NO_3} and maximum F_{NO_3} to the euphotic zone are summarized in the tables (e-h).

Figure 7 (a) Vertically integrated chlorophyll a (mg chl a m^{-2}) and (b) primary production ($\text{mg C m}^{-2} \text{d}^{-1}$). Values are proportional to the diameter of the circles. (c) Distribution of maximum nitrate flux to the euphotic zone (F_{NO_3} , $\text{mmol N m}^{-2} \text{d}^{-1}$) and (e) f-ratios for the euphotic zone (colours, no unit).

Figure 8 Time series station over 36h at the shelf edge. (a,b) Tidal current speed cubed, ctd-measurements (c, e, g, h) of potential temperature, salinity, oxygen and Brunt Väisälä frequency, respectively. Turbulence measurements of (d) dissipation rate of TKE and (f) calculated vertical turbulent diffusion coefficient. Observations are shown with small gray bullets and samples for water chemistry is shown with bullets in (g)s.

- 5 **Figure 9** Sketch of conditions across the shelf edge zone during summer. The largest f-ratios are found above the shelf-edge zone where the nutricline (D_{NO_3}) gets in contact with elevated mixing near the bottom. Deep waters are characterized by high nitrate concentration whereas surface water and water above the shallow North Sea (NS) are nitrate depleted.

Table 1. Distribution of photosynthetic parameters. Median values, and absolute median deviations (number of samples n in parenthesis) of photosynthetic parameters at 5 m below the surface and at the SCM.

Depth level	Depth [m]	P_{max}^B [$\mu\text{g C } (\mu\text{g Chl h})^{-1}$]	P_{max} [$\mu\text{g C } (\mu\text{g Chl h})^{-1}$]	α^B $10^{-2} \cdot [\mu\text{g C} \cdot (\mu\text{g Chl h } \mu\text{E m}^{-2} \text{ s}^{-1})^{-1}]$	β^B $10^{-3} \cdot [\mu\text{g C } (\mu\text{E m}^{-2} \text{ s}^{-1} \text{ h})^{-1}]$	E_{max} [$\mu\text{E m}^{-2} \text{ s}^{-1} \text{ h}$]	Chl a [mg chl m^{-3}]
Surface	5.0 ± 0.0 (23)	4.76 ± 1.33 (19)	5.48 ± 0.87 (23)	4.10 ± 0.90 (23)	1.70 ± 1.70 (23)	413 ± 76 (19)	0.16 ± 0.06 (23)
SCE	27.0 ± 5.0 (25)	1.72 ± 0.38 (24)	2.33 ± 0.64 (25)	2.70 ± 0.80 (25)	3.00 ± 0.90 (25)	192 ± 26 (24)	1.67 ± 0.73 (25)

Table 2 Median values, and absolute median deviations in three depth intervals of depth, depth of maximum nitrate flux (Depth_{max}), maximum nitrate flux into the euphotic zone (FNO3_{max}), depth of nutricline (D_{NO_3}), vertically integrated chlorophyll a (Chl_{int}) and primary production (PP).

Depth interval (m)	Depth (m)	Depth_{max} (m)	FNO3_{max} ($\text{mmol N m}^{-2} \text{ d}^{-1}$)	D_{NO_3} (m)	Chl_{int} (mg chl a m^{-2})	PP ($\text{mg C m}^{-2} \text{ d}^{-1}$)
50 - 80	65 ± 6 (25)	39 ± 3 (25)	0.05 ± 0.04 (25)	34.5 ± 4.5 (28)	34.8 ± 13.3 (69)	476 ± 138 (69)
80 - 130	97 ± 11 (18)	43 ± 3 (18)	0.11 ± 0.07 (18)	34.5 ± 3.5 (20)	26.4 ± 2.9 (24)	419 ± 41 (24)
> 130	263 ± 58 (30)	32 ± 5 (30)	0.06 ± 0.03 (30)	26.5 ± 4.0 (31)	26.6 ± 4.2 (35)	528 ± 101 (35)

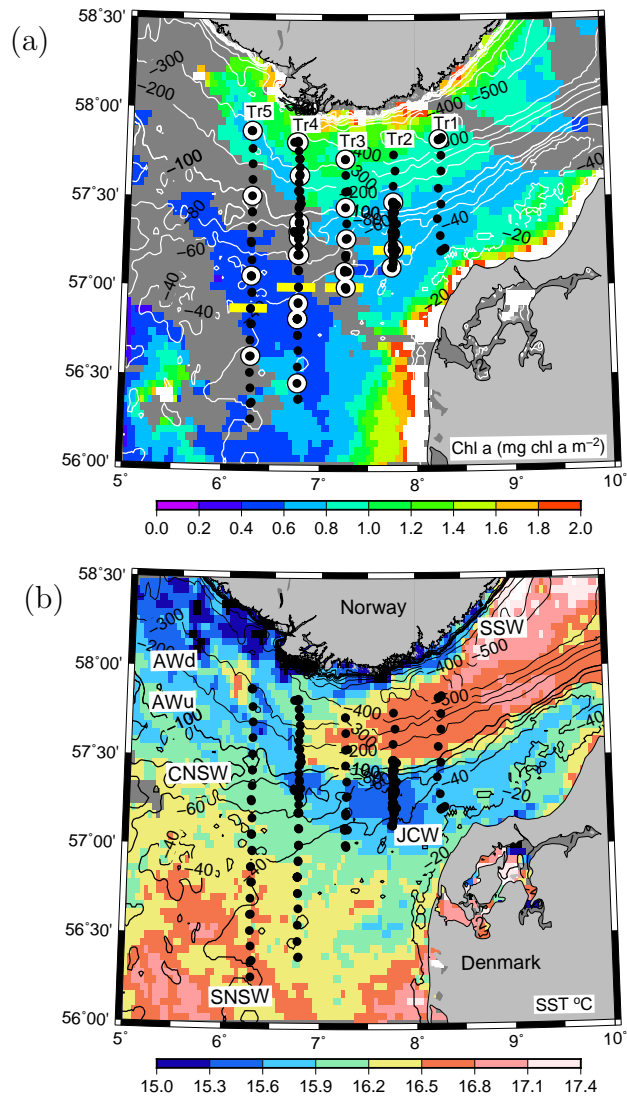


Figure 1

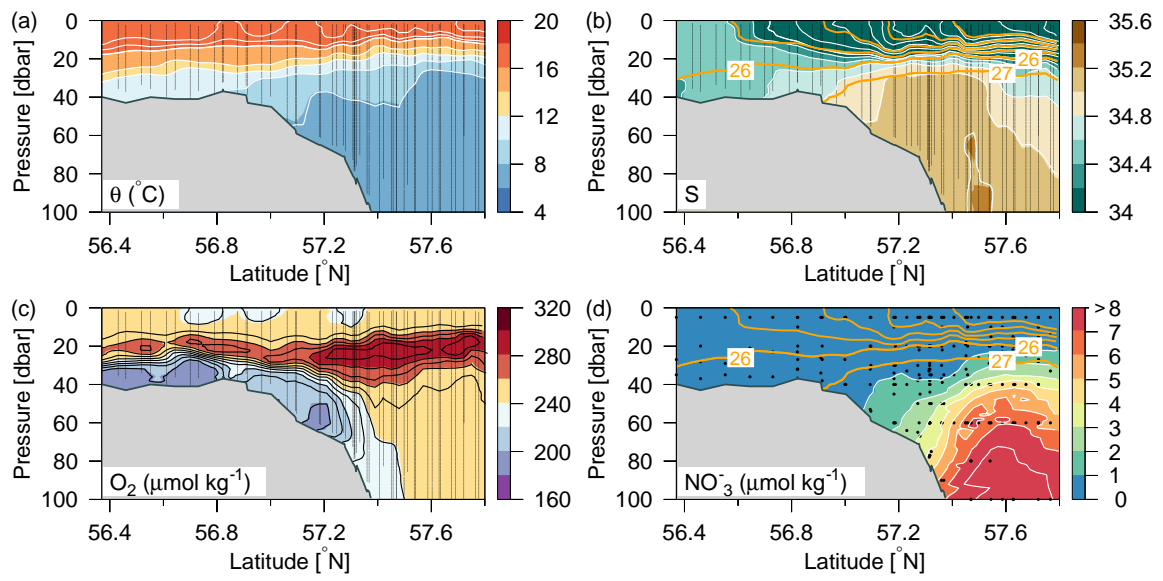


Figure 2

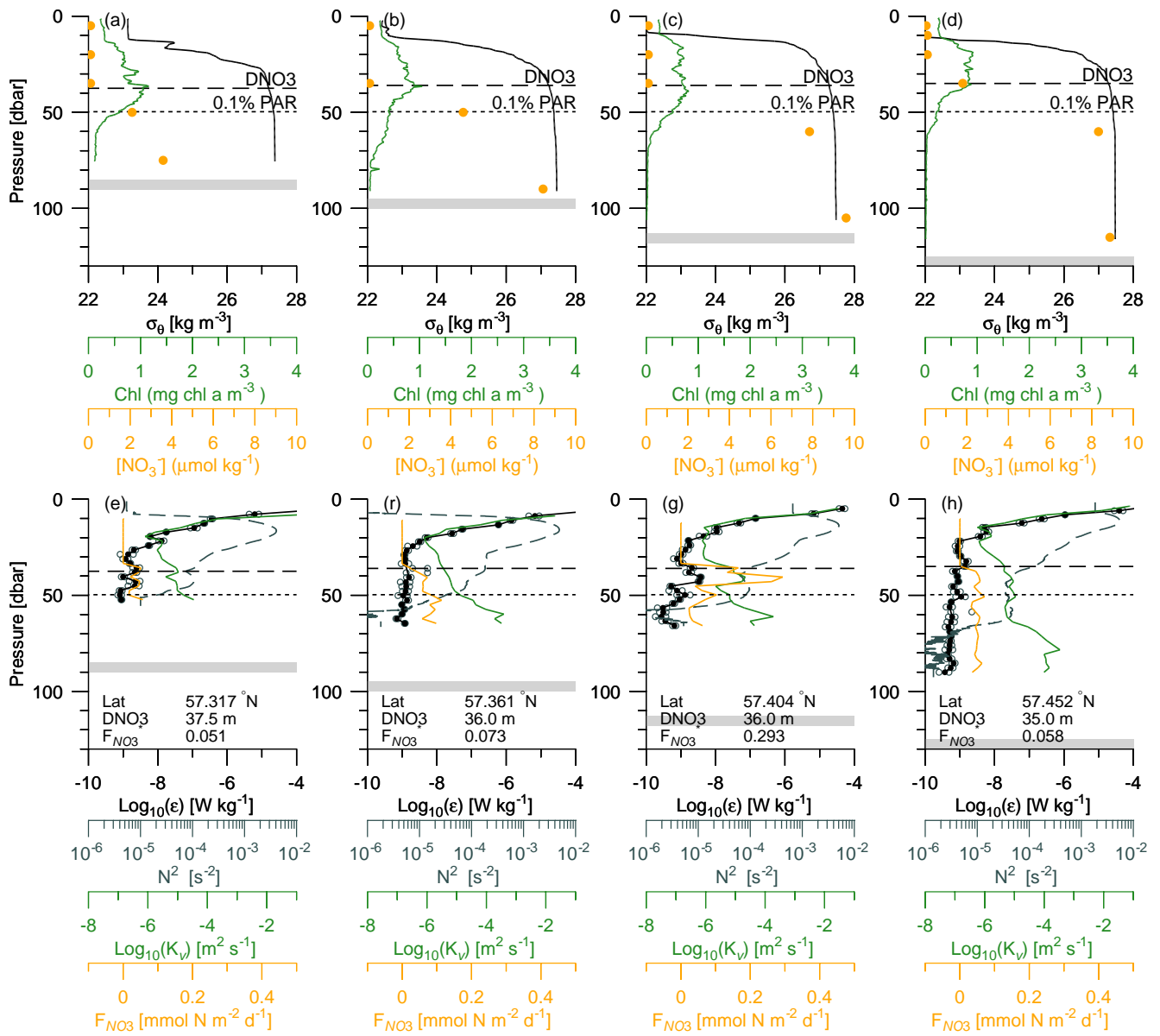


Figure 6

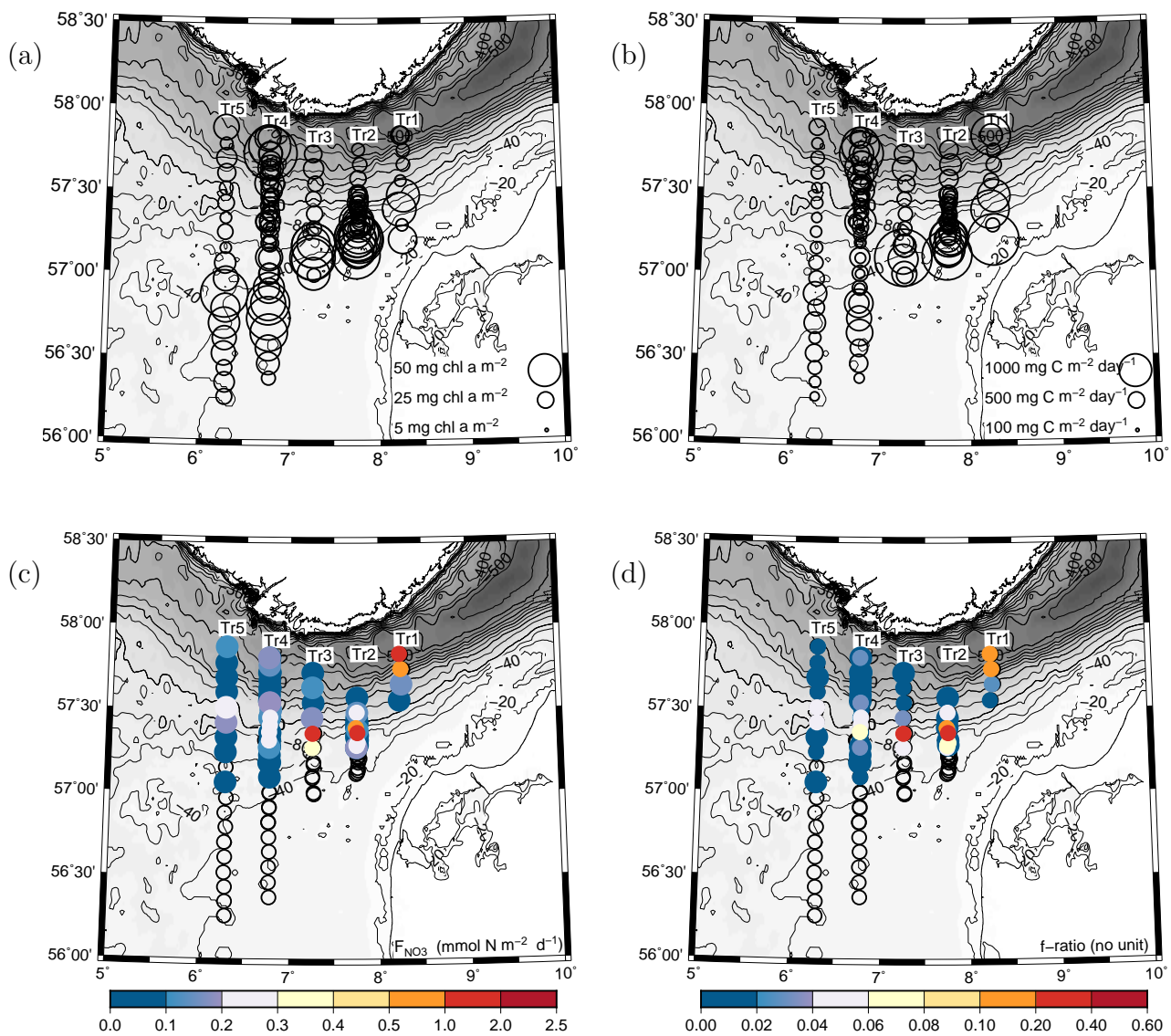


Figure 7

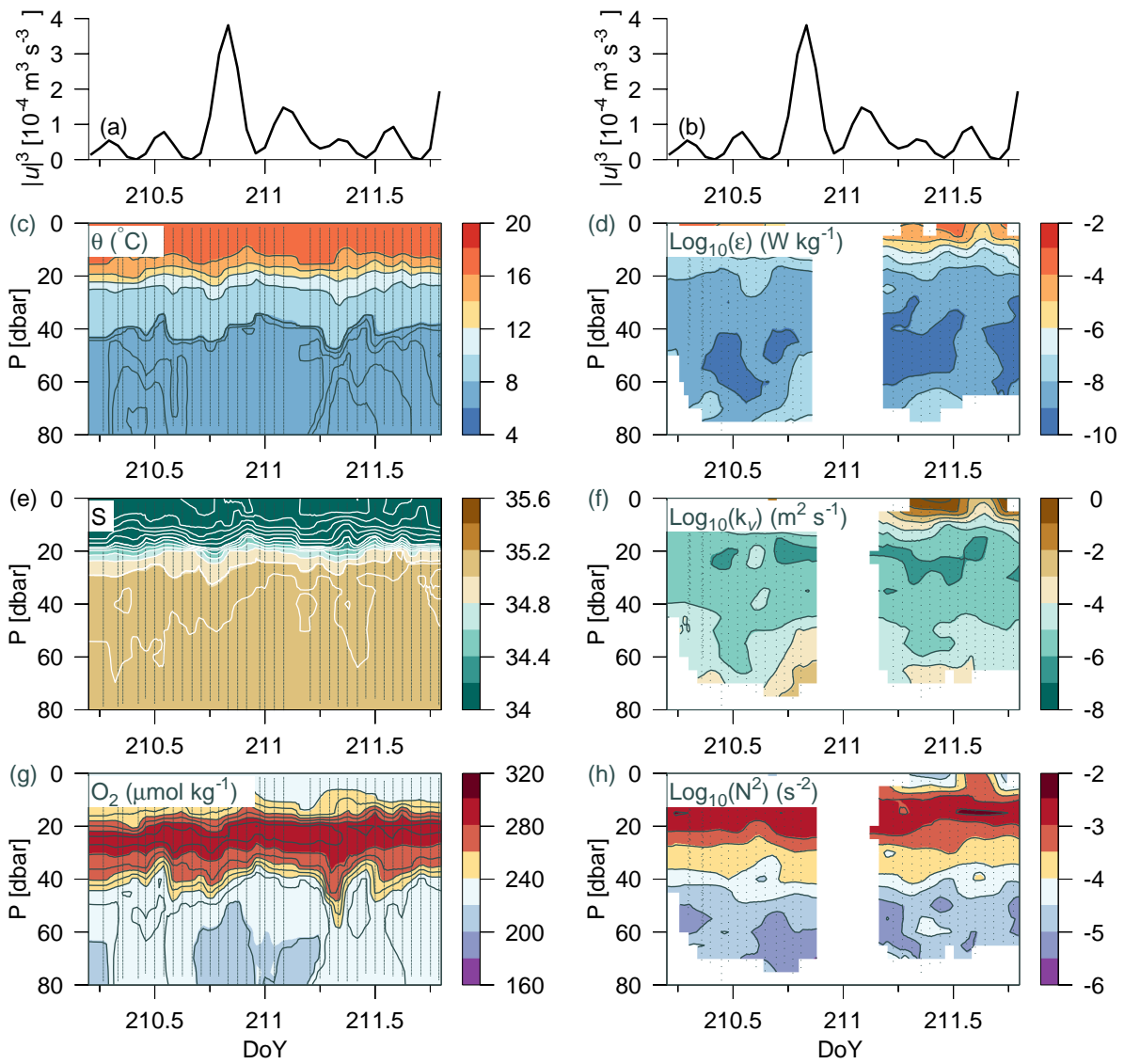


Figure 8

Supplementary material

Analysis of turbulence variation and uncertainty

Temporal variation and uncertainty associated with the shear probe measurements were assessed at a time series station, T1, located on Tr2 (57.287 °N, 7.758 °E; 62 m deep) starting 20 July 23:25 and ending 21 July 21:44 (Fig. S1). In total, 107 profiles were made to ~50 m depth in three sequences during the period with typically ~3 minutes between each cast. The temporal variation showed a modest change in temperature between 10-20 m (Fig. S1a) and a relatively small dissipation of turbulent kinetic energy (TKE) at mid-depth during the first 6 hours of the measurements (Fig. S1b). The instrument was equipped with two shear probes and the dissipation of TKE (ϵ) was calculated from each of the probes. The difference between these two estimates, made across the same water volume, are analysed below to assess the uncertainty of the ϵ -values.

Samples above 15 m were disregarded in the error-analysis to avoid any influence from the movement of the ship. The relative difference between the calculated dissipation of TKE (ϵ) obtained from each of the two shear probes (i.e., ϵ_1 and ϵ_2) was calculated as: $\Delta\text{Log}_{10}\epsilon = \text{Log}_{10}(\epsilon_1) - \text{Log}_{10}(\epsilon_2)$. In total, there were 1145 pairs over the 22h period with a relatively small $\Delta\text{Log}_{10}\epsilon$ average value of -0.063 and a standard and absolute deviation of 0.23 and 0.14, respectively. We applied the absolute deviation, i.e. the more conservative estimate, as being representative of the uncertainty of the ϵ -values. The relative probability distribution of $\Delta\text{Log}_{10}\epsilon$ showed a qualitative accordance with a normal distribution characterised by the average value and absolute deviation (Fig. S1b), although the error-distribution showed a tendency to a broader variance for $\Delta\text{Log}_{10}\epsilon$ larger than ~0.4. This was also clear from the cumulative probability distribution (Fig. S1d) where the error-distribution deviated from a normal distribution (confirmed by a Kolmogorov-Smirnov test). We considered the largest values of $\Delta\text{Log}_{10}\epsilon$ to indicate sources of errors which could not be directly related to the instrument but potentially associated with the measurement procedure, for example influence from the rope on the free-falling instrument (all casts were made with free and undisturbed line to the free falling instrument during the whole cast). Therefore, we applied the criterion that only measurements where $\Delta\text{Log}_{10}\epsilon$ was less than 3 times the absolute deviation (i.e. 0.42) were considered to be acceptable and these were included in the analysis. This criterion eliminated only a small number of the ϵ -values from the data set.

Temporal variation was also considered from the time series measurements at T1. Variation of ϵ is expected to vary due to tides, wind, breaking internal waves etc. Therefore, variations at a single time series station cannot be expected to be representative for the data set as a whole. However, the short-term temporal variation was analysed from samples of ϵ binned in 5 m intervals and analysed over a period of 30 minutes (i.e. 11 casts) resulting in average values and absolute standard deviations of 1.6 ± 0.6 , 1.4 ± 0.6 and 2.1 ± 1.0 in depth intervals between 25-30m, 30-35m and 35-40m, respectively (in units of $10^{-9} \text{ W kg}^{-1}$). Thus, short term variation was relatively small and temporal changes between subsequent casts were considered to have a small influence on the calculated ϵ -values. Therefore, ϵ -values were, in general, derived from a single cast between the relatively closely spaced stations, where the ϵ -value obtained by averaging the calculated value from the two probes was reported. In addition to the time series station, T1, a similar time series station (T2) located at Tr4 is discussed in the text.

Supplementary figure legends

Figure S1 Turbulence measurements from time series station, T1, located on Tr2 (57.287 °N, 7.758 °E) starting 20 July 23:25 and ending 21 July 21:44. (a) Temperature (°C) and (c) turbulent kinetic energy dissipation (ϵ , W kg^{-1}) were measured in 107 profiles (small bullets) in three sequences during the 22h period and are shown as a function of pressure and time (Day of the Year). (b) The error-distribution ($\Delta\text{Log}_{10}\epsilon$ in units of $\text{Log}_{10}(\text{W kg}^{-1})$, see text) between calculated ϵ from the two shear probes (gray bars) and the normal distribution (green) associated with the average and absolute deviation of the error-distribution. (d) The cumulative probability of the error-distribution (black) compared with the associated normal distribution (green).

Figure S2 Distributions along the five transects of (a) vertically integrated chlorophyll a (mg chl a m^{-2}), (b) primary production ($\text{mg C m}^{-2} \text{d}^{-1}$), (c) nutricline depth (m), (d) maximum nitrate flux into the euphotic zone ($\text{mmol N m}^{-2} \text{d}^{-1}$) and (e) f-ratio in euphotic zone. Repeated stations on Tr2 and Tr4, separated in time by about a week, are shown with bullets and open circles.

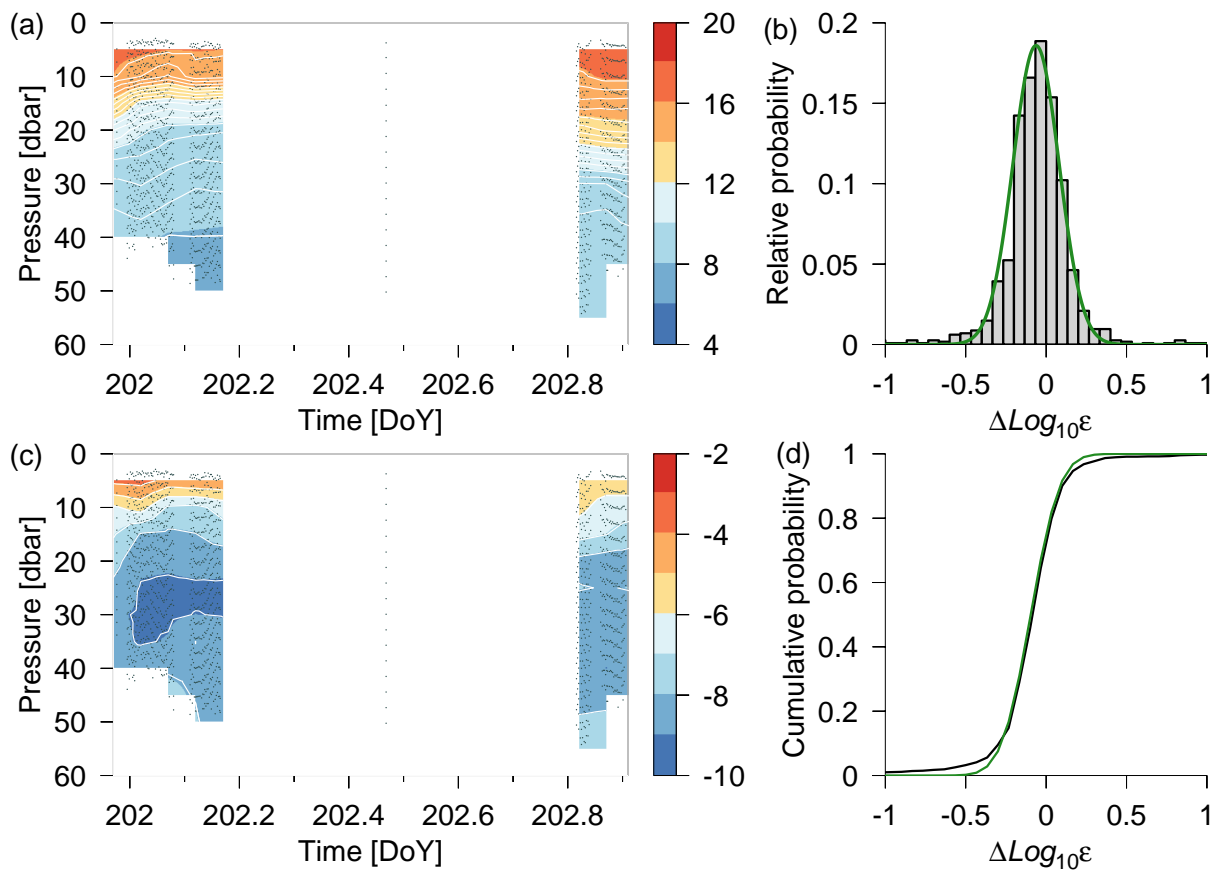


Figure S1